Ruthenium and osmium carbonyl clusters incorporating stannylene and stannyl ligands

Shariff E. Kabir,* [a] Arun K. Raha,[a] Mohammad R. Hassan,[a] Brian K. Nicholson,* [b] Edward Rosenberg,* [c] Ayesha Sharmin,[c] Luca Salassa[c]

[a] *Department of Chemistry, Jahangirnagar University, Savar, Dhaka 1342, Bangladesh*

[b] *Department of Chemistry, University of Waikato, Hamilton, New Zealand*

[c] *Department of Chemistry, The University of Montana, Missoula, Montana 59812, USA*

Summary

The reaction of $[Ru_3(CO)_{12}]$ with Ph_3SnSPh in refluxing benzene furnished the bimetallic Ru-Sn compound $[Ru_3(CO)_8(\mu-SPh)_2(\mu_3-SnPh_2)(SnPh_3)_2]$ **1** which consists of a $SnPh_2$ stannylene bonded to three Ru atoms to give a planar tetra-metal core, with two peripheral $SnPh_3$ ligands. The stannylene ligand forms a very short bond to one Ru atom [Sn-Ru 2.538(1) Å] and very long bonds to the other two [Sn-Ru 3.074(1) Å]. The germanium compound $[Ru_3(CO)_8(\mu-SPh)_2(\mu_3-GePh_2)(GePh_3)_2]$ **2** was obtained from the reaction of $[Ru_3(CO)_{12}]$ with Ph_3GeSPh and has a similar structure to that of **1** as evidenced by spectroscopic data. Treatment of $[Os_3(CO)_{10}(MeCN)_2]$ with Ph_3SnSPh in refluxing benzene yielded the bimetallic Os-Sn compound $[Os_3(CO)_9(\mu-SPh)(\mu_3-SnPh_2)(MeCN)(\eta^1-C_6H_5)]$ **3**. Cluster **3** has a superficially similar planar metal core, but with a different bonding mode with respect to that of **1**. The Ph_2Sn group is bonded most closely to Os(2) and Os(3) [2.7862(3) and 2.7476(3) Å respectively] with a significantly longer bond to Os(1), 2.9981(3) Å indicating a weak back-donation to the Sn. The reaction of the bridging dppm compound $[Ru_3(CO)_{10}(\mu-dppm)]$ with Ph_3SnSPh afforded $[Ru_3(CO)_6(\mu-dppm)(\mu_3-S)(\mu_3-SPh)(SnPh_3)]$ **5**. Compound **5** contains an open triangle of Ru atoms simultaneously capped by a sulfido and a PhS ligand on opposite sides of the cluster with a dppm ligand bridging one of the Ru-Ru edges and a Ph_3Sn group occupying an axial position on the Ru atom not bridged by the dppm ligand.

Introduction

Recently, bimetallic cluster complexes have attracted great interest because of their use as precursors to bimetallic nanoparticles by gentle thermolysis on high surface area mesoporous supports and have been shown to be superior catalysts for hydrogenation reactions.[1] Tin[2-5] and germanium[6] are widely used to modify and enhance the activity of bimetallic catalysts leading to increased selectivity in a variety of chemical transformations.[2] There is also evidence that tin can assist in the binding of metallic nanoparticles to oxide supports when used in heterogeneous catalysis. [3-5,7] Oxidative addition of $R_3M'H$ ($M' = Si$, Sn or Ge; R = Et, Bu or Ph) to the lightly stabilized $[M_3(CO)_{12-n}(NCMe)_n]$ (n = 1 or 2) gives mixed metal clusters of the type $[M_3(CO)_{11}(M'R_3)(\mu-H)]$ and $[M_3(CO)_{10}(CH_3CN)(M'R_3)(\mu-H)]$ (M = Ru, Os; $M' = $ Ge, Sn; R = Me, Et, Bu or Ph).[8] It has also been reported that the unsaturated $[Os_3(CO)_{10}(\mu-H)_2]$ reacts analogously with $R_3M'H$ giving $[Os_3(CO)_{10}(M'R_3)(\mu-H)_3]$[9]. Adams et al. recently reported that reactions of Ph_3SnH with metal carbonyl cluster complexes leads to the formation of polynuclear metal carbonyl complexes containing μ-$SnPh_2$, μ_3-SnPh, or μ_4-Sn ligands by the cleavage of phenyl groups.[10] For example, the high-nuclearity bimetallic Ru-Sn cluster compounds, $[Ru_5(CO)_{10}(SnPh_3)(\mu-SnPh_2)_4(\mu_5-C)(\mu-H)]$ and $[Ru_5(CO)_7(SnPh_3)(\mu-SnPh_2)_4(\mu_5-C)(\mu-H)]$, containing five tin ligands are formed from the reactions of $[Ru_5(CO)_{15}(\mu_5-C)]$ or $[Ru_5(CO)_{12}(C_6H_6)(\mu_5-C)]$ with Ph_3SnH.[10a] Very recently the bimetallic complexes $[Os_3(CO)_{11}(SnPh_3)(\mu-H)]$ and $[Os_3(CO)_9(\mu-SnPh_2)_3]$ were reported from the reaction of $[Os_3(CO)_{12}]$ with Ph_3SnH. These complexes undergo reaction across the Os-Sn bond with $Pt(PBu^t_3)_2$ to yield $[Os_3(CO)_9\{Pt(PBu^t_3)\}(\mu-SnPh_2)_3]$ and $[Os_3(CO)_9\{Pt(Ph)(PPh_3)_2\}(\mu-SnPh_2)_2(\mu_3-SnPh)]$ by insertion of a $Pt(PPh_3)_2$ group into one of the Sn-Ph bonds.[10d,f] Thermolysis of $[Os_3(CO)_{11}(SnPh_3)(\mu-H)]$ under a CO atmosphere gives $[Os_3(CO)_{12}(Ph)(\mu_3-SnPh_3)]$ and $[Os_4(CO)_{16}(\mu_4-Sn)]$.[10e] In recent studies we have found that both the electronically unsaturated $[Os_3(CO)_8(Ph_2PCH_2P(Ph)C_6H_4)(\mu-H)]$ and electron precise $[Os_3(CO)_{10}(\mu-dppm)]$ react with Ph_3SnH to yield a series of novel Os-Sn complexes.[11] As far as we are aware, no examples of transition metal bimetallic clusters containing sulfur-metal and tin-metal bonds in the same molecule have been reported. It

occurred to us that the presence of a potentially capping sulfur ligand could induce the stannyl moieties to adopt new bonding modes in the resulting bimetallic clusters. We have now investigated the reactions of tetraphenylthiostannane with [Ru₃(CO)₁₂], [Os₃(CO)₁₀(MeCN)₂] and [Ru₃(CO)₁₀(μ-dppm)]. The objectives were to synthesize bimetallic complexes with sulfur and tin ligands in unusual bonding modes which could be used as precursors to nanoconductors, because the presence of two functionalities in one molecule proffers an extended π-electron system with possible metal-metal interactions. Besides the structural characterization the electronic structures of these compounds were investigated by DFT calculations and also the electrochemical properties of the products were studied in an attempt to gain a further understanding of how changes in the bonding mode of the ligands to a trimetallic core impacts its electron acceptor-donor properties.

Results and discussion

The reaction of [Ru₃(CO)₁₂] with Ph₃SnSPh in refluxing benzene resulted in the isolation of the bimetallic cluster [Ru₃(CO)₈(μ-SPh)₂(μ₃-SnPh₂)(SnPh₃)₂] **1** in 18% yield (Scheme 1). Characterization of **1** was by X-ray crystallography and spectroscopic data.

$$Ru_3(CO)_{12} \quad + \quad Ph_3XSPh \quad \xrightarrow{80\ ^oC}$$

X = Sn, **1**
X = Ge, **2**
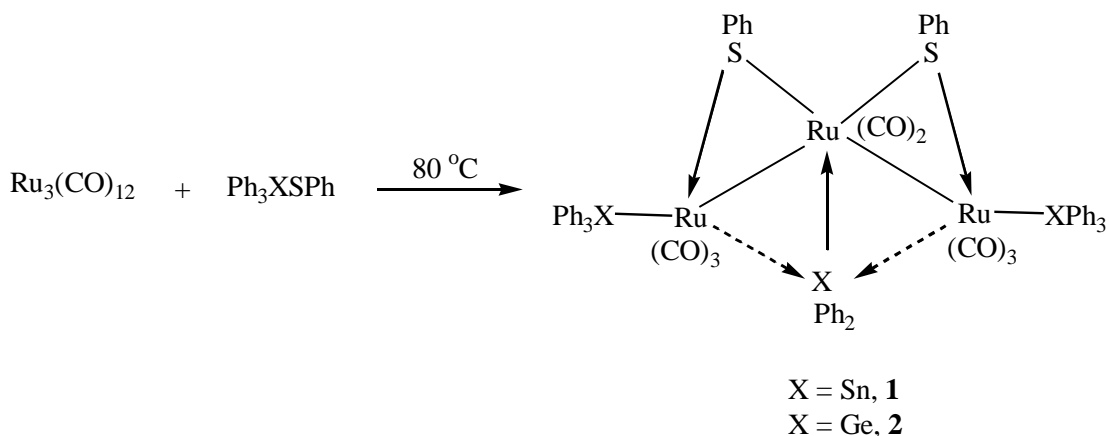
Scheme 1

The structure of the cluster is illustrated in Figure 1, with selected parameters given in the caption. The molecule consists of three Ru atoms, each bonded to the SnPh₂ group to give a planar tetra-metal core. Each of the Ru-Ru edges is bridged by a μ-SPh group, positioned to give shorter distances to the outer Ru atoms. There is a terminal Ph₃Sn group attached to the

outer Ru atoms, with remaining coordination sites occupied by CO ligands. The terminal Ph$_3$Sn groups have a normal Sn-Ru bond length of 2.682(1) Å. The most unusual feature is the bonding of the Ph$_2$Sn group. This forms a very short 2.538(1) Å link to Ru(2), and extremely long bonds to Ru(1) and Ru(3) (av. 3.074(1) Å). A search of the Cambridge Crystallographic Database[12] for Sn-Ru bonds where there is also at least one Sn-C bond shows a range of 2.60-2.76 Å. Therefore the Ru(2)-Sn(3) bond in **1** represents an unusually short Ru-Sn bond while the Ru(1)-Sn(3) and Ru(3)-Sn(3) bonds are borderline non-bonding. This suggests that the Ph$_2$Sn group can be considered as a singlet stannylene, forming a strong σ-donor bond via its sp^2 lone pair of electrons to Ru(2), and is stabilized by weak back-donation to the Sn from Ru(1) and Ru(3) . This can be represented formally as shown in Scheme 1.

This representation also accommodates the unsymmetrical bonding of the SPh groups, and gives a formal eighteen-electron count for each of the Ru atoms. R$_2$Sn ligands bonded as a stannylene in mononuclear complexes have been long-known when R is a very bulky group, as in [{(Me$_3$Si)$_2$HC}$_2$SnCr(CO)$_5$] and other related examples[13], but this type of bonding for R$_2$Sn in polymetallic compounds is unusual, because in transition metal clusters these normally bridge a metal-metal bond as part of a closed triangle[10d, 14]. The closest analogues are from Adam's group[10d,15], where some Re-Pt and Os-Pt clusters incorporate a five-coordinate Ph$_2$Sn ligand related to that in **1**, but where the bond distances to the three metal atoms are much more uniform.

The spectroscopic data of **1** are fully consistent with the solid-state structure. Despite the very different chemical environments for the Ph$_3$Sn and Ph$_2$Sn groups, the ^{119}Sn NMR spectrum of **1** showed only a small difference in chemical shift, with signals at δ –25.3 and -29.9 respectively relative to SnMe$_4$. The FAB mass spectrum showed the molecular ion peak at m/z 1719. The electrospray mass spectrum of **1** in MeOH (with added NaOMe to aid ionisation[16]) gave not only a weak peak corresponding to the expected [M+OMe]$^-$, but also one assignable to [M]$^-$ through reduction in the mass spectrometer source, a relatively rare ionization process. The main signal was at *m/z* 1369 which corresponds to [M-SnPh$_3$]$^-$, arising from remarkably facile loss of the Ph$_3$Sn$^+$ group in the mass spectrometer.

Although there have been major efforts to prepare Ru-Sn and Os-Sn bimetallic cluster complexes in recent years, to date few examples of ruthenium carbonyl cluster complexes

containing germanium ligands have been reported.[17] Adams *et al.*[18] have very recently shown that $[M_4(CO)_{12}(\mu-H)_4]$ (M = Os, Ru) react with Ph_3GeH leading to the formation of $[M_4(CO)_{10-n}(\mu_4-GePh)_2(\mu-GePh_2)_{2+n}]$ (where M = Ru, n = 0, 1, 2, and where M = Os, n = 1, 2) containing an unusually large number of phenylgermanium ligands. To see whether Ph_3GeSPh can engage in a similar reaction to that of Ph_3SnSPh we have investigated its reaction with $[Ru_3(CO)_{12}]$. Treatment of $[Ru_3(CO)_{12}]$ with Ph_3GeSPh in refluxing benzene resulted in the isolation of $[Ru_3(CO)_8(\mu-SPh)_2(\mu_3-GePh_2)(GePh_3)_2]$ **2** in 15% yield (Scheme 1). Formation of compound **2** is proposed on the basis of elemental analysis, mass spectral data and the similarity of the IR and NMR data to **1**. The infrared spectrum of **2,** in the carbonyl region is very similar to that of **1** and the proton NMR shows a similar pattern in the aromatic region to **1** indicating that they are isostructural. The FAB mass spectrum of **2** exhibits a molecular ion peak at m/z 1581 consistent with its formulation.

The reaction of $[Os_3(CO)_{10}(NCMe)_2]$ with Ph_3SnSPh in refluxing benzene resulted in the isolation of $[Os_3(CO)_9(\mu-SPh)(\mu-SnPh_2)(NCMe)(\eta^1-C_6H_5)]$ **3** in 27% yield (Scheme 2). Compound **3** has been characterized by a combination of spectroscopic data and single crystal X-ray diffraction studies.
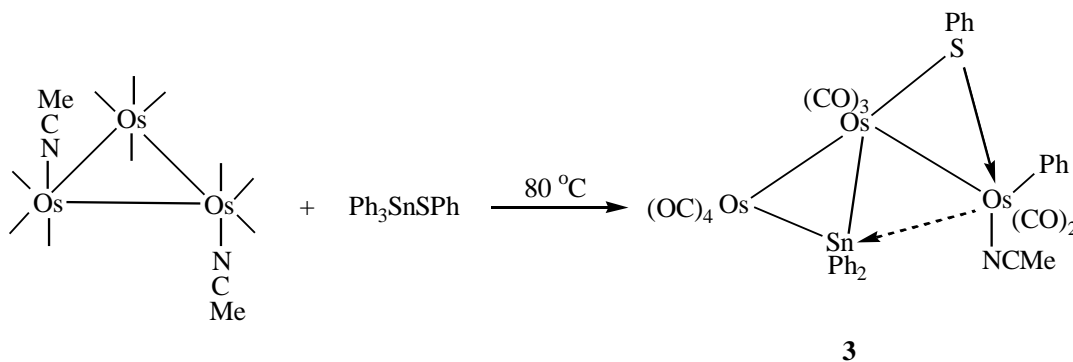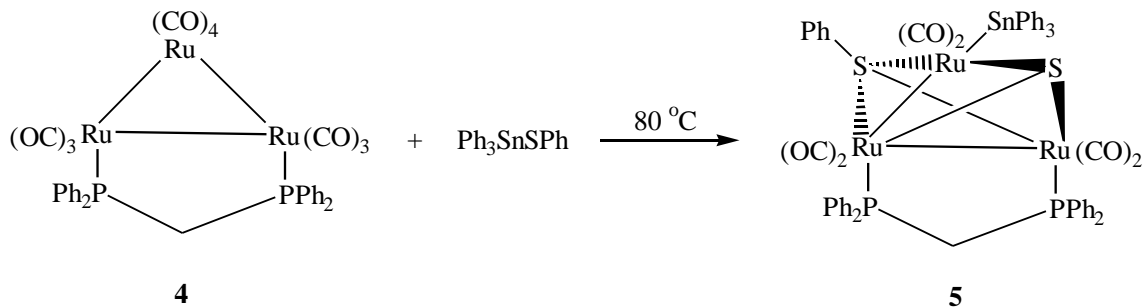

Scheme 2

The Os_3Sn cluster **3** has a superficially similar metal core to that of **1**, but the details are different. As shown in Figure 2, again there is a planar array for the metal atoms, but the Ph_2Sn group is bonded most closely to Os(2) and Os(3) [2.7862(3) and 2.7476(3) Å respectively] with a significantly longer bond to Os(1), 2.9981(3) Å. One of the Os-Os bonds is also bridged by the PhS ligand and is longer [Os(1)-Os(2) = 3.039 Å] than the unbridged

Os(2)-Os(3) at 2.999 Å. Both of these are at the longer end of the range of Os-Os bonds reported in the literature. Os(1) is also attached to a terminal phenyl group, and to a MeCN ligand. Overall the bonding in cluster **3** is formally represented as drawn in Scheme 2. The closest analog for this cluster is $[Os_3(\mu_3\text{-}SnCl_2)(\mu\text{-}CH_2)(CO)_{11}]$, reported by Geoffroy's group[19]. This has a $SnCl_2$ in place of the Ph_2Sn in **2**, and a bridging methylene instead of a μ-SPh, but is otherwise similar. For this earlier example the different Os-Sn bond lengths form a similar pattern to that found for **2**, though all are shorter as expected with more electronegative Cl substituents on the tin atom. The Os-Os bonds are very similar in both examples. The spectroscopic data for **3** are fully consistent with the solid-state structure. The FAB mass spectrum shows the molecular ion peak at m/z 1323. The electrospray mass spectrum of **3** in MeOH shows clean signals assignable to both $[M+OMe]^-$ at m/z 1354 and $[M+OMe\text{-}MeCN]^-$ at m/z 1313 under mild conditions (cone voltage <20 V), indicating a labile NCMe group. Loss of CO ligands only took place at cone voltages > 50 V. In addition to the phenyl proton resonances, the ^{1}H NMR spectrum contains a singlet at δ 1.69 assigned to the methyl protons of the coordinated NCMe ligand.

Treatment of $[Ru_3(CO)_{10}(\mu\text{-}dppm)]$ (**4**) with Ph_3SnSPh in refluxing benzene afforded $[Ru_3(CO)_6(\mu\text{-}dppm)(\mu_3\text{-}S)(\mu_3\text{-}SPh)(SnPh_3)]$ **5** in 54% yield (Scheme 3), which has been characterized by a combination of spectroscopic data and single crystal X-ray diffraction studies.

Scheme 3

The structure of **5** is given in Figure 3, which shows a completely different species to that obtained from the same reaction with $[Ru_3(CO)_{12}]$. In this case the Ph_3Sn group remains

intact and is coordinated to one Ru atom. The three Ru atoms form an open triangle bridged on one side by a PhS$^-$ ligand, and on the other by an S^{2-} one. An alternative view, emphasised in Figure 3, is as a Ru$_3$S$_2$ square-pyramidal cluster core, with a dppm bridging one Ru-Ru edge, a Ph$_3$Sn group occupying an axial position on the other Ru atom, and with a Ph group in an equatorial site on one of the S atoms. The six CO ligands, each rurhenium atom containing two, complete the coordination. An interesting feature is the sulfido and the SPh ligands, formed by cleavage of C-S and Sn-S bonds of the ligand, respectively, which asymmetrically cap the Ru$_3$ system [S(2)-Ru(1) = 2.4476(6), S(2)-Ru(2) = 2.4432(6), S(2)-Ru(3) = 2.4746(6) Å and S(1)-Ru(1) = 2.3562(6), S(1)-Ru(2) = 2.4130(6), S(1)-Ru(3) = 2.3371(6) Å]. Of the two Ru-Ru bonds, the Ru(2)-Ru(3) distance of 2.7481(3) Å supported by the bridging dppm ligand is significantly shorter than the unsupported Ru(1)-Ru(2) distance of 2.9030(3) Å. The former is also significantly shorter than the corresponding dppm bridged Ru-Ru distance in [Ru$_3$(CO)$_{10}$(μ-dppm)] [(2.834(1) Å].[20]

The spectroscopic data of **5** in solution are consistent with the solid-state structure. In addition to the phenyl proton resonances of the triphenyltin, capping PhS and bridging dppm ligands, the ^{1}H NMR spectrum in the aliphatic region exhibits two multiplets at δ 4.18 and 3.70 due to the diastereotopic methylene protons of the dppm ligand. The ^{31}P{^{1}H} NMR spectrum of exhibits two doublets at δ 32.6 (J = 88.1 Hz) and –13.2 (J = 88.1 Hz), implying inequivalent ^{31}P nuclei of the dppm ligand. The ^{119}Sn NMR spectrum of **5** shows a similar shift for the Ph$_3$Sn group as in the case of **1**, with a signal at δ -28.6 showing a 15 Hz coupling to one P atom of the dppm ligand, which is consistent with the structure found by X-ray crystallography. The FAB mass spectrum shows the molecular ion peak at m/z 1348. The electrospray mass spectra gave a clean [M+Na]$^+$ signal centred at *m/z* 1371 in positive ion mode, and an [M-H]$^-$ peak at *m/z* 1347 arising from abstraction of a methylene H from the dppm ligand, a common ionisation process for dppm-substituted clusters.[16, 21] Both of these ions were remarkably robust, undergoing CO loss only at high cone voltages, >60 V, and in contrast to the very ready loss of Ph$_3$Sn$^+$ from **1**, there was no indication at all of a similar process for **5**.

The cyclic voltamograms for clusters **1** and **5** in dichloromethane show irreversible reduction waves at -1.22 and -1.37 V and irreversible oxidation waves at +1.12 and +0.87 V respectively relative to the ferrocene/ferrocenium ion couple. That cluster **5** shows a more

negative reduction and more positive oxidation half wave potential can be attributed to the presence of the electron donating properties of the dppm but the significant difference in their structure make even this conclusion tentative.

Calculation of the optimized geometries of complexes **1** and **3** was performed in order to gain some further insight into the nature of the bonding between the Sn and the Ru or Os atoms in the metal core. All calculations were performed using the Gaussian 03 package.[22] Geometry optimization of the two clusters was obtained with a two-level ONIOM procedure,[23] in which the B3PW91/LANLD2Z[24a] (D95V[24b] for first row atoms) was used as higher level (QM) and the UFF molecular mechanics force field[25] was employed as lower level (MM) of theory. No negative frequencies where found for the two optimized geometries. Energies and orbitals for **1**, **3** and **5** were obtained by performing a single-point calculation at the B3PW91/LANLD2Z for heavy atoms and at the B3PW91/6-31G**[26] for the light atoms. This approach yielded very good agreement with experimentally determined metal-metal bond lengths but the metal sulfur bond lengths were significantly elongated with respect to the observed values (Table 2 and 3). This elongation of metal ligand bond lengths is often observed when an *f* polarization is not applied to the metals as is the case here.[27] For the purposes of comparing the nature of the metal based orbitals this approach is adequate and saved considerable computational time. The HOMO orbital in **1** is highly localized in the Ru_3Sn plane and shows a particularly dense bonding region between the stannylene Sn(3) and the central Ru atom, Ru(2) (Figure 4a). The HOMO orbital for **3** is also localized in the Os_3Sn metal core but has electron density in more out of plane regions and involves the Os(2)-SPh and Os(3)-SPh moieties (Figure 5a). These differences are in agreement with the observed very short Ru(2)-Sn(3) bond length relative to the other Sn-Ru bonds in **1**, while in **3** the related Os(2)-Sn(1) bond is only slightly shorter than the other two Os-Sn interactions (Table 3). The LUMO orbital for **1** is metal based and shows a bonding region in the area of Ru(1)-Sn(3)-Ru(3) while the LUMO for **3** is mainly localized on Os(1) and Os (2) and is antibonding in nature (Figure 5b). This is in agreement with the larger HOMO-LUMO gap observed for **5** (0.136 eV, 1096 cm^{-1}) relative to **1** ((0.095 eV, 766 cm^{-1}).

Conclusions

In summary, bimetallic compounds $[Ru_3(CO)_8(\mu\text{-SPh})_2(\mu_3\text{-SnPh}_2)(SnPh_3)]$ **1**, $[Ru_3(CO)_8(\mu\text{-SPh})_2(\mu_3\text{-GePh}_2)(GePh_3)]$ **2**, $[Os_3(CO)_9(\mu\text{-SPh})(\mu\text{-SnPh}_2)(MeCN)(\eta^1\text{-}C_6H_5)]$ **3** and $[Ru_3(CO)_6(\mu\text{-dppm})(\mu_3\text{-S})(\mu_3\text{-SPh})(SnPh_3)]$ **5** have been synthesized and structurally characterized. Compounds **1** and **2** further expand the chemistry involving the multiple additions of tin and germanium ligands to metal carbonyl cluster complexes. The new Ru-Sn, Ru-Ge and Os-Sn bimetallic clusters reported in this study should be useful precursors for the preparation of new heterogeneous nano-scale catalysts on supports. Of particular interest is the very short Ru-Sn bond observed in **1**. DFT calculations are consistent with this being a stannylene-Ru donor acceptor interaction. This bond would be expected to be particularly more reactive towards supports with Lewis acid character providing an initial binding site for eventual nano-catalyst formation.

Experimental

General data

Unless otherwise stated all the reactions were performed under a nitrogen atmosphere using standard Schlenk techniques. Solvents were dried and distilled prior to use by standard methods. $[Ru_3(CO)_{12}]$ was purchased from Strem and $[Os_3(CO)_{10}(MeCN)_2]$[28] and $[Ru_3(CO)_{10}(\mu\text{-dppm})]$[29] were prepared according to the literature methods. Infrared spectra were recorded on a Shimadzu FTIR 8101 spectrophotometer. ^1H and $^{31}P\{^1H\}$ and NMR spectra were recorded on Bruker DPX 400 instruments. ^{119}Sn NMR spectra were recorded on a Bruker ACS 300 spectrometer. All chemical shifts are reported in δ units with reference to the residual protons of the deuterated solvents for proton, to external 85% H_3PO_4 for ^{31}P and $SnMe_4$ for ^{119}Sn chemical shifts. Elemental analyses were performed by Schwarzkopf Microanalytical Laboratories, Woodside, NY. Mass spectra were recorded on a Fisons Platform II ESI mass spectrometer, with MeOH as mobile phase and NaOMe added as an ionization aid.[16] The m/z values reported are the strongest in the isotope envelope, and formulations were confirmed by matching isotope patterns with simulated ones generated with ISOTOPE.[30] Fast atom bombardment mass spectra were obtained on a JEOL SX-102 spectrometer using 3-nitrobenzyl alcohol as matrix and CsI as calibrant.

Reaction of [Ru$_3$(CO)$_{12}$] with Ph$_3$SnSPh. To a benzene solution (30 cm^3) of [Ru$_3$(CO)$_{12}$] (100 mg, 0.16 mmol) was added Ph$_3$SnSPh (144 mg, 0.32 mmol) and the reaction mixture was heated to reflux at 80 ^{o}C for 45 min. The solvent was removed in vacuo and the residue chromatographed by TLC on silica gel. Elution with hexane/CH$_2$Cl$_2$ (4:1, v/v) developed two bands. The faster moving band gave unconsumed starting material (30 mg), while the slower moving band afforded [Ru$_3$(CO)$_8$(μ-SPh)$_2$(μ_3-SnPh$_2$)(SnPh$_3$)$_2$] **1** (51 mg, 18%) as blue-red crystals after recrystallization from hexane/CH$_2$Cl$_2$ at -4^oC. Anal. Calc. for C$_{68}$H$_{50}$O$_8$Ru$_3$S$_2$Sn$_3$: C, 47.52; H, 2.93. Found: C, 47.71, H, 3.11. IR (υ_{CO}, CH$_2$Cl$_2$): 2090 w, 2052 m, 2043m, 2023 vs, 1998 m cm^{-1}. ^{1}H NMR (CDCl$_3$): δ7.77-6.73 (m, 50H);. ^{119}Sn NMR (CDCl$_3$): δ -25.3 (s, 2Sn, Ph$_3$Sn); -29.9 (s, 1Sn, Ph$_2$Sn) ppm. FAB MS: *m/z* 1719 [M]$^+$. ESI-MS: *m/z* 1750 [M+OMe]$^-$, 1719 [M]$^-$, 1369 [M-SnPh$_3$]$^-$.

Reaction of [Ru$_3$(CO)$_{12}$] with Ph$_3$GeSPh. A similar reaction to that above between [Ru$_3$(CO)$_{12}$] (100 mg, 0.16 mmol) with Ph$_3$GeSPh (129 mg, 0.31 mmol) in benzene (30 cm^3) followed by similar chromatographic separation developed two bands. The faster moving band gave unconsumed starting material (37 mg, 37%), while the slower moving band afforded [Ru$_3$(CO)$_8$(μ-SPh)$_2$(μ-GePh$_2$)(GePh$_3$)$_2$] **2** (36 mg, 15%) as deep red crystals after recrystallization from hexane/CH$_2$Cl$_2$ at -4^oC. Anal. Calc. for C$_{68}$H$_{50}$O$_8$Ru$_3$S$_2$Ge$_3$: C, 51.68; H, 3.19. Found: C, 51.71, H, 3.13. :IR (υ_{CO}, CH$_2$Cl$_2$): 2092 w, 2056 m, 2045 m, 2021 vs, 1996 m cm^{-1}. ^{1}H NMR (CDCl$_3$): δ 8.32 - 6.48 (m 50H).

Reaction of [Os$_3$(CO)$_{10}$(MeCN)$_2$] with Ph$_3$SnSPh. A benzene solution (75 mL) of [Os$_3$(CO)$_{10}$(MeCN)$_2$] (180 mg, 0.19 mmol) and Ph$_3$SnSPh (87 mg, 0.19 mmol) was refluxed for 7 h. Workup as described above afforded [Os$_3$(CO)$_9$(μ-SPh)(μ-SnPh$_2$)(MeCN)(η^1-C$_6$H$_5$)] **3** (69 mg, 27%) as yellow crystals from hexane/CH$_2$Cl$_2$ at -4^oC. Anal. Calc. for C$_{35}$H$_{23}$N$_1$O$_9$Os$_3$S$_1$Sn$_1$: C, 31.77; H, 1.75. Found: C, 31.82; H, 1.72%. IR (υ_{CO}, CH$_2$Cl$_2$) 2098 m, 2058 w, 2024 vs, 2013 s, 1986 m, 1965 w cm^{-1}. ^{1}H NMR (CDCl$_3$): δ 8.07-6.99 (m, 20H), 1.69 (s, 3H). FAB MS: *m/z* 1323 [M]$^+$. ESI-MS: *m/z* 1354 [M+OMe]$^-$, 1313 [M+OMe-MeCN]$^-$.

Reaction of [Ru₃(CO)₁₀(μ-dppm)] with Ph₃SnSPh. Ph₃SnSPh (142 mg, 0.31 mmol) was added to a benzene solution (50 cm³) of [Ru₃(CO)₁₀(μ-dppm)] **4** (100 mg, 0.10 mmol). The reaction mixture was heated to reflux for 30 min during which time the color changed from orange to deep red. A similar chromatographic separation to that above yielded [Ru₃(CO)₆(μ-dppm)(μ₃-S)(μ₃-SPh)(SnPh₃)] **5** (75 mg, 54%) as yellow crystals from hexane/CH₂Cl₂ at −4°C. Anal. Calc. for $C_{55}H_{42}O_6P_2Ru_3S_2Sn_1$: C, 49.04; H, 3.14. Found: C, 49.10; H, 3.17%. IR (v_{CO}, CH₂Cl₂) 2019 m, 2004 vs, 1986 s, 1952 s cm⁻¹. ¹H NMR (CDCl₃): δ 7.75-6.97 (m, 40H), 4.18 (m, 1H), 3.70 (m, 1H). ³¹P{¹H} NMR (CDCl₃): δ 32.6 (d, J = 88.1 Hz), −13.2 (d, J = 88.1 Hz). ¹¹⁹Sn NMR (CDCl₃): δ −28.6 [d, $^3J(^{31}P-^{119}Sn)$ = 15 Hz]. FAB MS: m/z 1348 [M]⁺, ESI-MS: m/z (negative ion mode) 1379 [M+OMe]⁻, 1347 [M-H]⁻; (positive ion mode) 1371 [M+Na]⁺.

X-ray Crystallography.

X-ray intensity data were collected on a Bruker SMART CCD diffractometer with Mo-Kα X-rays using standard procedures and software. Semi-empirical absorption corrections were applied (SADABS).[31] Structures were solved by direct methods and developed and refined on F^2 using the SHELX programmes[32] operating under WinGX.[33] Hydrogen atoms were included in calculated positions.

Electrochemistry

Electrochemical measurements were performed using a BAS CV-50W analyzer equipped with a standard three-electrode cell. The cell was designed to allow the tip of the reference electrode to approach closely to the working electrode. Voltammetric experiments were performed using aqueous Ag/AgCl as a reference electrode, a glassy carbon as a working electrode and platinum wire as the auxiliary electrode. Potential data are referenced to the ferreocene(0/+) couple, which is oxidized in CH₂Cl₂ at +0.48 V vs Ag/AgCl. Typically, a solution containing 1 mM of the cluster and 0.1 M supporting electrolyte (tetrabutylammonium hexafluorophosphate, Bu₄NPF₆) was prepared using freshly distilled dichloromethane. The solution was degassed prior to introducing the sample and also between runs. Positive feedback *i*R compensation was routinely applied.

Computational Details

All calculations were performed using the Gaussian 03 package.[22] Geometry optimization of the two clusters was obtained with a two-level ONIOM procedure,[23] in which the B3PW91/LANLD2Z[24a] (D95V[24b] for first row atoms) was used as higher level (QM) and the UFF molecular mechanics force field[25] was employed as lower level (MM) of theory. No negative frequencies where found for the two optimized geometries. Energies and orbitals for **1**, **3** and **5** were obtained by performing a single-point calculation at the B3PW91/LANLD2Z for heavy atoms and at the B3PW91/6-31G**[26] for the light atoms.

Supplementary information

Crystallographic data for the structural analyses have been deposited with the Cambridge Crystallographic Data Center, CCDC Nos. 661316-661318 for compounds **1**, **3** and **5**. Copies of this information may be obtained free of charge from the Director, CCDC, 12 Union Road, Cambridge, CB2 1 EZ, UK (fax: +44-1223-336033; e-mail: deposit@ccdc.cam.ac.uk or www: http://www.ccdc.ac.uk).

Acknowledgements

References

1 (*a*) J. M. Thomas, R. Raja and D. W. Lewis, *Angew. Chem., Int. Ed.*, 2005, **44**, 6456; (*b*) J. M. Thomas, B. F. G. Johnson, R. Raja, G. Sankar and P. A. Midgley, *Acc. Chem. Res.*, 2003, **36**, 20; (*c*) J. M. Thomas, R. Raja, B. F. G. Johnson, S. Hermans, M. D. Jones and T. Khimyak, *Ind. Eng. Chem. Res.*, 2003, **42**, 1563; (*d*) B. F. G. Johnson, *Top. Catal.*, 2003, **24**, 147.

2 (*a*) S. M. Santos, A. M. Silva, E. Jordao and M. A. Fraga, *Catal. Commun*. 2004, **5**, 377; (*b*) S. Hermans, R. Raja, J. M. Thomas, B. F. G. Johnson, G. Sankar and D.

Gleson, *Angew. Chem., Int. Ed.*, 2001, **40**, 1211; (*c*) S. Hermans and B. F. G. Johnson, *J. Chem. Soc., Chem. Commun.*, 2000, 1955.

3 (*a*) R. Burch, *J. Catal.*, 1981, **71**, 348; (*b*) R. Burch and L. C. Garla, *J. Catal.*, 1981, **71**, 360; (*b*) R. Srinivasan and B. H. Davis, *Platinum Met. Rev.*, 1992, **36**, 151; (*c*) T. Fujikawa, F. H. Ribeiro and G. A. Somorjai, *J. Catal.* 1998, **178**, 58.

4 (*a*) G. W. Huber, J. W. Shabaker and J. A. Dumesic, *Science*, 2003, **300**, 2075; (*b*) M. S. Holt, W. L. Wilson and J. H. Nelson, *Chem. Rev.*, 1989, **89**, 11.

5 B. F. G. Johnson, S. A. Raynor, D. B. Brown, D. S. Shephard, T. Mashmeyer, J. M. Thomas, S. Hermans, R. Raja and G. Sankar, *J. Mol. Catal. A: Chem.*, 2002, **182-183**, 89.

6. (a) G. Lafaye, C. Micheaud-Especel, C. Montassier, P. Marecot, Appl. Catal. A, 2002, **230**, 19; (b) B. Didillon, J. P. Candy, F. Lepepetier, O. A. Ferretti and J. M. Basset, Stud. Surf. Sci. Catal., 1993, 78, 147; (c) (a) G. Lafaye, C. Mihut, C. Especel, M. D. Amiridis. Langmuir, 2004, **20**, 10612.

7 A. Hungria, R. Raja, R. D. Adams, B. Captain, J. M. Thomas, P. A. Midgley, V. Golvenko and B. F. G. Johnson, *Angew. Chem., Int. Ed.*, 2006, **45**, 969.

8 (*a*) K. Burgess, C. Guerin, B. F. G. Johnson and J. Lewis, *J. Organomet. Chem.*, 1985, **295**, C3; (*b*) W. K. Leong, R. K. Pomeroy, R. J. Batchelor, F. W. B. Einstein and C. F. Campana, *Organometallics*, 1996, **15**, 1582.

9 (*a*) R. J. Hall, P. Serguievski and J. B. Keister, *Organometallics*, 2000, **19**, 4499; (*b*) F. W. B. Einstein, R. K. Pomeroy and A. C. Willis, *J. Organomet. Chem.,* 1986, **311**, 257.

10 (*a*) R. D. Adams, B. Captian, W. Fu and M. D. Smith, *Inorg. Chem.*, 2002, **41**, 5593; (*b*) R. D. Adams, B. Captian, W. Fu and M. D. Smith, *Inorg. Chem.*, 2002, **41**, 2302; (*c*) R. D. Adams, B. Captain, J. L. Smith, M. B. Hall, C. L. Beddie, C. E. Wedster, W. Fu and M. D. Smith, *Inorg. Chem.*, 2004, **43**, 7576; (*d*) R. D. Adams, B. Captain, and L. Zhu, *Organometallics*, 2006, **25**, 2049; (e) R. D. Adams, B. Captain and L. Zhu, *Organometallics*, 2006, **25**, 4183; (f) R. D. Adams, B. Captain and L. Zhu, *Inorg. Chem.*, 2007, **46**, 4605.

11 M. R. Hassan, G. Hogarth, G. M. G. Hossain, S. E Kabir, A. K. Raha, M. S. Saha and D. A. Tocher, *Organometallics*, 2007, **26**, 6473.

12   Cambridge Crystallographic Database, V5.28 + updates, 2007; F. H. Allen, *Acta Cryst.*, 2002, **B58**, 380.

13   J. D. Cotton, P. J. Davidson, D. E. Goldberg, M. F. Lappert and K. M. Thomas, *J. Chem. Soc.*, *Chem. Commun.*, 1974, 893.

14   (*a*) R. F. Gerlach, K. M. Mackay and B. K. Nicholson, *Rev. Silicon, Germanium, Tin and Lead Compounds*, 1981, **5**, 67; (*b*) K. M. Mackay and B. K. Nicholson, in Ch 43, G. Wilkinson, F. G. A. Stone and E. W. Abel (Eds), Comprehensive Organometallic Chemistry, Pergamon, Oxford, 1982; (*c*) W. K. Leong, F. W. B. Einstein and R. K. Pomeroy, *Organometallics*, 1996, 1582; (*d*) C. J. Cardin, D. J. Cardin, M. A. Convery, Z. Dauter, D. Fenske, M. M. Devereux and M. B. Power, *J. Chem. Soc., Dalton Trans.*, 1996, 1133; (*e*) R. D. Adams, B. Captain , W. Fu and M. B. Smith, *J. Organomet. Chem.*, 2003, **671**, 158.

15   (*a*) R. D. Adams, B. Captain, R. H. Herber, K. Johansson, I. Nowik, J. L. Smith and M. D. Smith, *Inorg. Chem.*, 2005, **44**, 6346; (*b*) R. D. Adams, B. Captain, K. Johansson and J. L. Smith, *J. Am. Chem. Soc.*, 2005, **127**, 488.

16   W. Henderson, J. S. McIndoe, B. K. Nicholson and P. J. Dyson, *J. Chem. Soc., Dalton Trans.*, 1998, 519.

17   (*a*) J. A. K. Howard and P. Woodward, J. Chem. Soc., A, 1971, 3648; (*b*) Y. Zhang, B. Wang, S. Xu and X. Zhou *Organometallics*, 2001, **20**, 3829; (*c*) R. D. Adams, B. Captain and W. Fu, *Inorg. Chem.,* 2003, **42**, 1328; (*d*) R. D. Adams, B. Captain and W. Fu, *J. Organomet. Chem.* 2003, **671**, 158; (e) R. D. Adams, B. Captain and W. Fu, *Inorg. Chem.,* 2005, **44**, 6623.

18   R. D. Adams, E. M. Boswell, B. Captian and M. A. Patel, *Inorg. Chem.*, 2007, **46**, 533; see also R. D. Adams, B. Captain, and E. Trufan, *J. Cluster Sci.*, 2007, **18**, 642.

19   N. Viswanathan, E. D. Morrison, G. L. Geoffroy, S. J. Geib, and A. L. Rheingold, *Inorg. Chem.*, 1986, **25,** 3100.

20.   A. W. Coleman, D. F. Jones, P. H. Dixneuf, C. Brisson, J. –J. Bonnet and G. Lavigne, *Inorg. Chem.*, 1984, **23**, 952.

21   e.g. see A. B. Antonova, M. I. Bruce, P. A. Humphrey, M. Gaudio, B. K. Nicholson, N. Scoleri, B. W. Skelton, A. H. White and N. N. Zaitseva, *J. Organomet. Chem.*, 2006, **691**, 4694.

22   (*a*) F. Maseras and K. Morokuma, *J. Comput. Chem.*, 1995, **16**, 1170. (*b*) S. Humbel, S. Sieber and K. Morokuma, *J. Chem. Phys.* **1996**, *105*, 1959-1967.

23   A. K. Rappé, C. J. Casewit, K. S. Colwell, W. A. Goddard and W. M. Skiff, *J. Am. Chem. Soc.* 1992, **114**, 10024.

24   (*a*) P. J. Hay and W. R. Wadt, *J. Chem. Phys.*, 1985, **82**, 270. (*b*) T. H. Dunning Jr. and P. J. Hay, in Modern Theoretical Chemistry, Ed. H. F. Schaefer III, Vol. 3 (Plenum, New York, 1976, 1-28.

25   R. Ditchfield, W. J. Hehre, and J. A. Pople, *J. Chem. Phys.*, 1971, **54**, 724.

26   M. J. Frisch, G. W. Trucks, H. B. Schlegel, G. E. Scuseria, M. A. Robb, J. R. Cheeseman, J. A. Montgomery Jr., T. Vreven, K. N. Kudin, J. C. Burant, J. M. Millam,S. S. Iyengar, J. Tomasi*, V. Barone, B. Mennucci, M. Cossi, G. Scalmani, N. Rega, G. A. Petersson, H. Nakatsuji, M. Hada, M. Ehara, K. Toyota, R. Fukuda, J. Hasegawa, M. Ishida, T. Nakajima, Y. Honda, O. Kitao, H. Nakai, M. Klene, X. Li, J. E. Knox, H. P. Hratchian, H. P., Cross, J. B., Adamo, C., Jaramillo, J., Gomperts, R., Stratmann, R. E., Yazyev, O., Austin, A. J., Cammi, R., Pomelli, C., Ochterski, J., Ayala, P. Y., Morokuma, K., Voth, G. A., Salvador, P., Dannenberg, J. J., Zakrzewski, V. G., Dapprich, S., Daniels, A. D., Strain, M. C., Farkas, O., Malick, D. K., Rabuck, A. D., Raghavachari, K., Forestman, J. B, Ortiz, J. V., Cui, Q., Baboul, A. G., Clifford, S., Cioslowski, J., Stefanov, B. B, Liu, G., Liashenko, A., Piskorz, P., Komaromi, I., Martin, R. L., Fox, D. J., Keith, T., Al-Laham, M. A., Peng, C. Y., Nanayakkara, A., Challacombe, M., Gill, P. M. W., Johnson, B., Chen, W, Wong, M. W., Gonzales, C., and Pople, J. A. Gaussian 03. (revision C.02). 2004. Wallingford CT, Gaussian Inc.

27.   D. G. Musaev, T. Nowroozi-Isfahani, K. Morokuma, E. Roseneberg, *Organometallics*, 2005, **24**, 5973.

28.   J. Lewis, P. J. Dyson, B. J. Alexander, B. F. G. Johnson, C. M. Martin, J. M. G. Nairn and E. Parsini, *J. Chem. Soc., Dalton Trans.*, 1993, 519.

29   M. I. Bruce, J. G. Matisons and B. K. Nicholson, *J. Organomet. Chem.*, 1983, **247**, 321.

30   L. J. Arnold, *J. Chem. Educ*., 1992, **69**, 811.

31   R. H. Blessing, Acta Cryst., 1995, **A51**, 33.

32   G. M. Sheldrick, SHELX97 *Programs for the solution and refinement of crystal structures*, University of Göttingen, Germany, 1997.

33 (*a*) L. J. Farrugia, WinGX, Version 1.70.01, University of Glasgow, UK; (*b*) L. J. Farrugia, J. Appl. Cryst., **32**, 1999, 837.

Table 1

Crystallographic data and structure refinement [a] for **1**, **3** and **5**

	1	**3**	**5**.CH_2Cl_2
Empirical formula	$C_{68}H_{50}O_8Ru_3S_2Sn_3$	$C_{35}H_{23}NO_9Os_3SSn$	$C_{55}H_{42}O_6P_2Ru_3S_2Sn$
Formula weight	1718.48	1322.89	1431.77
Crystal system	Triclinic	Monoclinic	Triclinic
Space group	$P\bar{1}$	$P2_1/n$	$P\bar{1}$
a, Å	13.826(1)	10.9339(2)	11.9706(3)
b, Å	13.944(1)	22.8143(2)	12.1970(3)
c, Å	17.434(1)	14.4812(2)	19.8844(5)
α, deg	73.71(1)	90	101.979(1)
β, deg	79.20(1)	95.212(1)	103.825(1)
γ, deg	82.45(1)	90	92.297(1)
Volume, Å^3	3157.9(4)	3597.4(1)	2745.1(1)
Z	2	4	2
D_{calc}, Mg/m^3	1.807	2.443	1.732
μ (Mo Kα), mm^{-1}	1.988	11.36	1.540
$F(000)$	1672	2424	1412
Crystal size, mm^3	0.28 x 0.26 x 0.20	0.28 x 0.24 x 0.20	0.28 x 0.18 x 0.16
θ_{max}/°	26.4	26.3	26.3
Index ranges	$-27 \leq h \leq 27$	$-18 \leq h \leq 18$	$-50 \leq h \leq 45$
	$0 \leq k \leq 38$	$-21 \leq k \leq 25$	$0 \leq k \leq 13$
	$0 \leq l \leq 16$	$0 \leq l \leq 27$	$0 \leq l \leq 56$
Reflections collected	29546	21313	26441
Independent reflections	12812 [R(int) = 0.031]	7303 [R(int) = 0.024]	11038 [R(int) = 0.020]
Max. and min. transmn	0.593 and 0.501	0.172 and 0.107	0.829 and 0.745
Parameters	757	452	649
Goodness-of-fit on F^2	1.155	1.110	1.015
R indices [$I>2\sigma(I)$]	$R_1 = 0.0452$	$R_1 = 0.0204$	$R_1 = 0.0224$
wR indices [all data]	$wR_2 = 0.0971$	$wR_2 = 0.0454$	$wR_2 = 0.0536$

[a] Details in common: X-radiation, Mo Kα (λ = 0.71073 Å), temperature (K) 89(2), refinement method: full-matrix least-squares on F^2.

Table 2.

Selected calculated and observed bond lengths and angles for compound **1**

Bond lengths (Å)	Calculated	Observed
Ru(1)-Ru(2)	2.9462	2.9020(7)
Ru(2)-Ru(3)	2.9466	2.9090(7)
Sn(1)-Ru(1)	2.7446	2.6832(6)
Sn(3)-Ru(1)	3.0835	3.0986(6)
Sn(3)-Ru(2)	2.5544	2.5380(7)
Sn(3)-Ru(3)	3.1032	3.0488(7)
Sn(2)-Ru(3)	2.7473	2.6808(7)
S(1)-Ru(1)	2.524	2.423(2)
S(1)-Ru(2)	2.523	2.348(2)
S(2)-(Ru(2)	2.5561	2.345(2)
S(2)-Ru(3)	2.5539	2.425(2)

Bond Angle (Degrees)		
Ru(1)-Ru(2)-Ru(3)	136.00	136.75(2)

Table 3.

Selected calculated and observed bond lengths and angles for compound **3**

<u>Bond lengths (Å)</u>

	Calculated	Observed
Os(1)-Os(2)	3.0557	3.0391(2)
Os(2)-Os(3)	2.9900	2.9990(2)
Os(1)-Sn((1)	3.1203	2.9981(3)
Os(2)-Sn(1)	2.8003	2.7862(3)
Os(3)-Sn(1)	2.8317	2.7476(3)
Os(2)-S(1)	2.565	2.386(1)
Os(1)-S(1)	2.546	2.405(1)
Os(1)-C(11)	2.123	2.135(4)

<u>Bond Angle (Degrees)</u>

Os(1)-Os(2)-Os(3)	121.568	117.836(7)

Captions to Figures.

Figure 1.

The structure of the cluster $[Ru_3(CO)_8(\mu\text{-SPh})_2(\mu_3\text{-SnPh}_2)(SnPh_3)]$ **1**, shown with 30% ellipsoids. Selected parameters: Ru(1)-Ru(2) 2.9020(7), Ru(2)-Ru(3) 2.9090(7), Sn(3)-Ru(1) 3.0986(7), Sn(3)-Ru(3) 3.0488(7), Sn(3)-Ru(2) 2.5380(7), Sn(1)-Ru(1) 2.6832(6), Sn(2)-Ru(3) 2.6808(7), S(1)-Ru(1) 2.423(2), S(1)-Ru(2) 2.348(2), S(2)-Ru(2) 2.345(2), S(2)-Ru(3) 2.425(2)Å; Ru(1)-Ru(2)-Ru(3) 136.75(2)°.

Figure 2.

The structure of the cluster $[Os_3(CO)_9(\mu\text{-SPh})(\mu\text{-SnPh}_2)(MeCN)(\eta^1\text{-C}_6H_5)]$ **3**, shown with 30% ellipsoids. Selected parameters: Os(1)-Os(2) 3.0391(2), Os(2)-Os(3) 2.9990(2), Sn(1)-Os(1) 2.9981(3), Sn(1)-Os(2) 2.7862(3), Sn(1)-Os(3) 2.7476(3), Os(1)-S(1) 2.405(1), Os(2)-S(1) 2.386(1), Os(1)-C(11) 2.135(4)Å; Os(1)-Os(2)-Os(3) 117.836(7)°.

Figure 3.

The structure of the cluster $[Ru_3(CO)_6(\mu\text{-dppm})(\mu_3\text{-S})(\mu_3\text{-SPh})(SnPh_3)]$ **5**, shown with 30% ellipsoids. Selected parameters: Ru(1)-Ru(2) 2.9030(3), Ru(2)-Ru(3) 2.7481(3), Sn(1)-Ru(1) 2.6139(3), S(1)-Ru(1) 2.3562(6), S(1)-Ru(2) 2.4130(6), S(1)-Ru(3) 2.3371(6), S(2)-Ru(1) 2.4476(6), S(2)-Ru(2) 2.4432(6), S(2)-Ru(3) 2.4746(6), P(1)-Ru(2) 2.3217(6), P(2)-Ru(3) 2.3202(6)Å; Ru(1)-Ru(2)-Ru(3) 85.63(1)°.

Figure 4.

HOMO (a) and LUMO (b) orbitals for compound **1**.

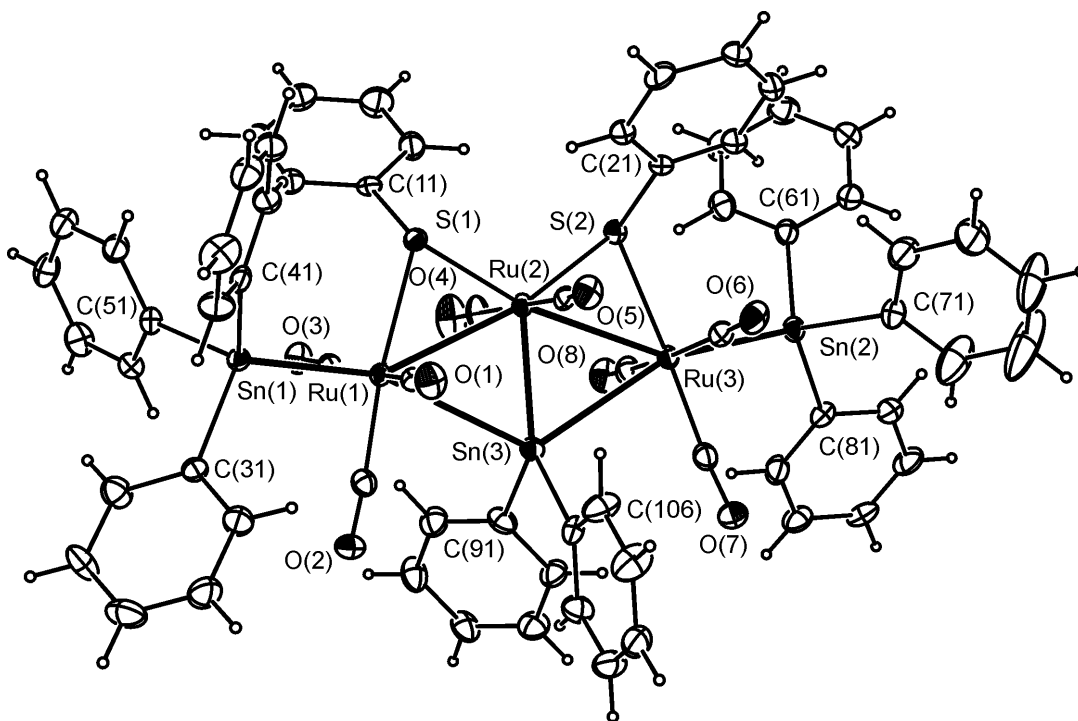Figure 5

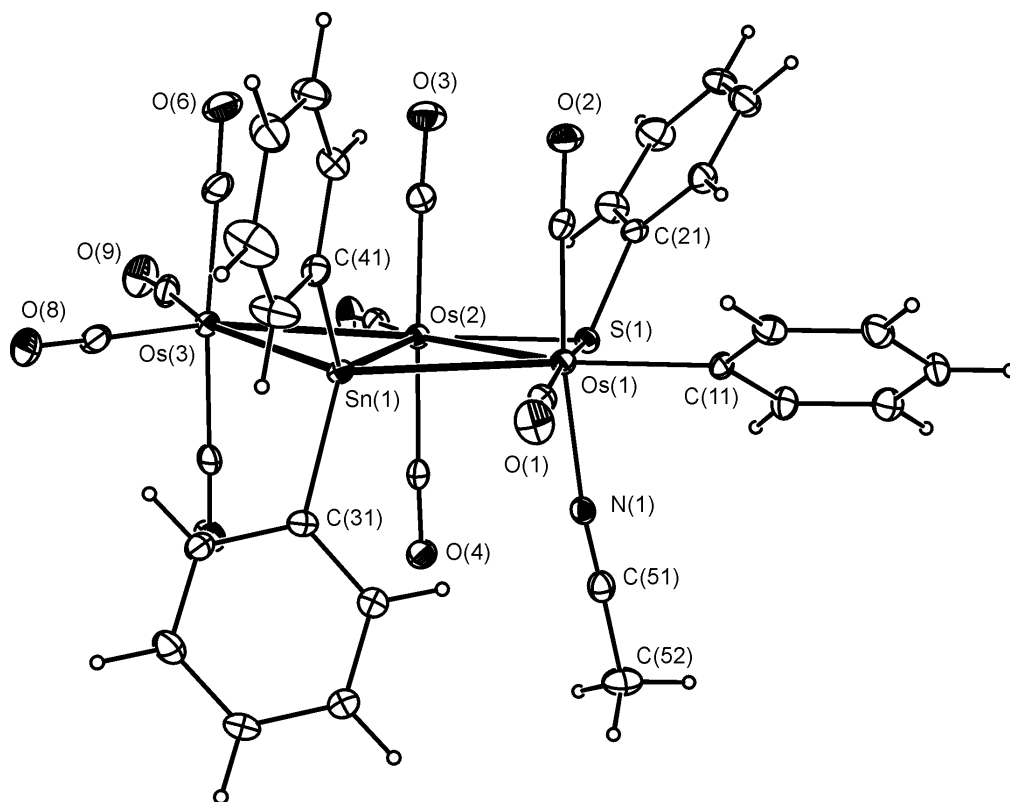HOMO (a) and LUMO (b) orbitals for compound **3**.

Figure 1

Figure 2
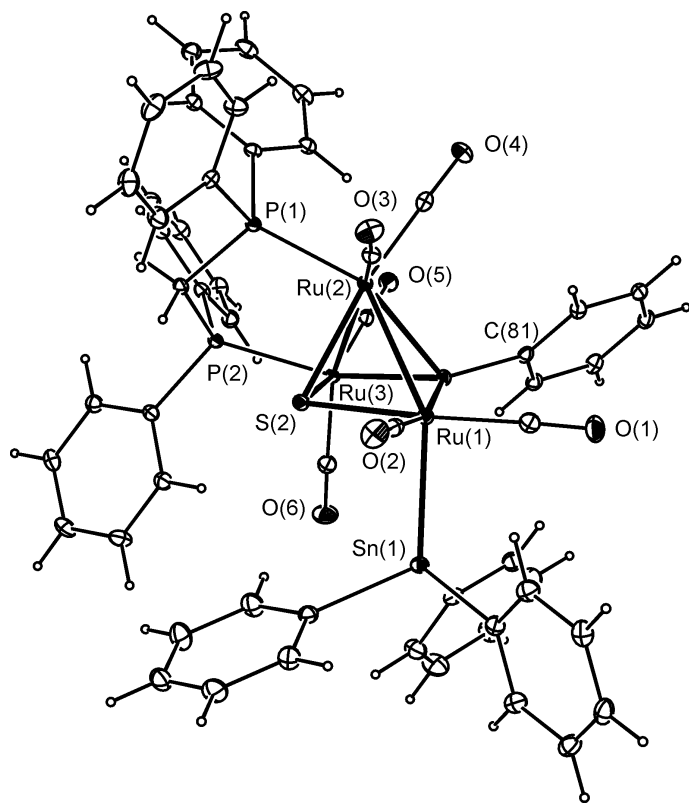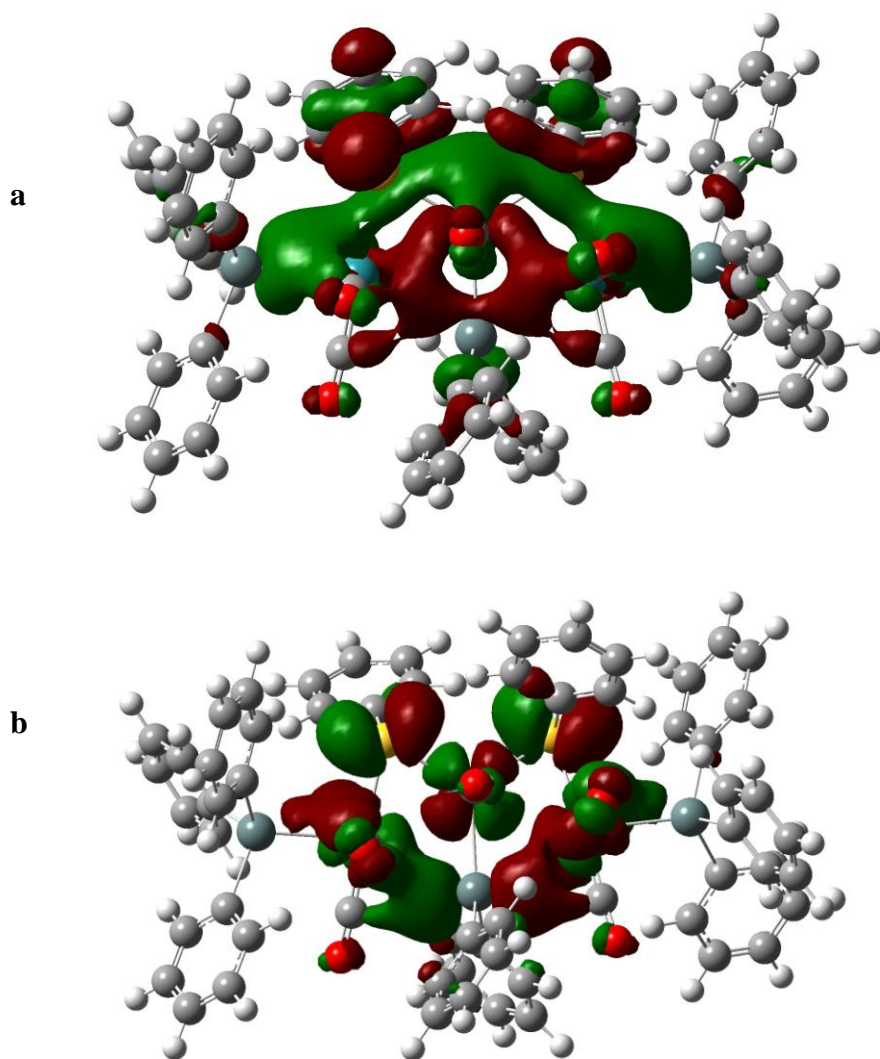
Figure 3

Figure 4

a

b

Figure 5